Geosat sea-level assimilation in a tropical Atlantic model using Kalman filter

Assimilation
Kalman filter
Altimetry
Tropical Atlantic

Assimilation
Filtre de Kalman
Altimétrie
Atlantique tropical

Lionel GOURDEAU [a], Sabine ARNAULT [b], Yves MÉNARD [a] and Jacques MERLE [b]

[a] Centre National d'Études Spatiales, Groupement de Recherche en Géodésie Spatiale, 18, avenue Edouard Belin, 31055 Toulouse Cedex, France.

[b] Laboratoire d'Océanographie Dynamique et de Climatologie (LODYC), Université Pierre et Marie Curie, Tour 14-2, boîte 100, 4, place Jussieu, 75252 Paris Cedex 5, France.

ABSTRACT

We present preliminary results on Geosat altimetric data assimilation in a linear vertical mode model of the tropical Atlantic Ocean. The Kalman filter technique is used to assimilate altimetric data along one track at a time as the satellite overflies the basin. Sensitivity and validation tests have been performed with simulated data. The results obtained with Geosat data are presented and compared on a monthly basis with objective analysis of altimetric data and oceanic general circulation model results.

Oceanologica Acta, 1992. **15**, 5, 567-574.

RÉSUMÉ

Assimilation par filtre de Kalman des données altimétriques de Geosat dans un modèle de l'Atlantique tropical

Cet article présente les premiers résultats obtenus par assimilation, à l'aide d'un filtre de Kalman, de données altimétriques de Geosat dans un modèle linéaire à mode vertical de l'Atlantique tropical. Les données sont assimilées trace par trace dans le modèle à l'instant du survol de la trace par le satellite. Des tests de sensibilité et de validation de la méthode ont d'abord été menés à partir de données simulées. Les résultats obtenus avec les mesures réelles sont présentés et discutés et comparés, en moyenne mensuelle, avec les cartes altimétriques construites par analyse objective ainsi qu'avec les résultats d'un modèle de circulation générale océanique.

Oceanologica Acta, 1992. **15**, 5, 567-574.

INTRODUCTION

It is now evident that tropical oceans play a key role in global climate evolution. However, the study of equatorial oceanic dynamics has been hampered by the lack of *in situ* conventional data. Recently, satellite data have offered to oceanographers a new approach for large-scale oceanic studies. They present an unexpected spatial and temporal coverage. But their processing, especially for altimetry in the tropics (*see* Arnault and Périgaud, this issue), requires a great deal of care.

On the other hand, numerical models constitute a further source of large-scale information (Philander and Pacanowski, 1986). However, results produced by such models suffer from uncertainties with regard to the forcings (winds, heat fluxes) or from inadequacies in their parametrizations (*e. g.* vertical diffusion; Schott and Boning, 1991). Therefore, combining satellite data together with models can lead to a better description of the ocean dynamics.

We investigate the variability of the tropical Atlantic dynamic topography by assimilating altimetric sea level anoma-

lies in a linear vertical mode model. There are several ways of assimilating data in a numerical model. Due to their easy implementation, polynomial adjustment or nudging have been used with complex oceanic models such as oceanic general circulation models [OGCM (Moore *et al.*, 1987; Derber and Rosati, 1989; Carton and Hackert, 1990; Leetma and Ji, 1989; Morlière *et al.*, 1989)]. Variational methods can also be employed (Scheinboum and Anderson, 1990). Most of these authors assimilate temperature profiles with objectives other than the description of the sea surface in mind. We chose to investigate a third type of approach which is both statistical and dynamic, using a complete Kalman filter with a simple but realistic numerical model previously employed by Bourles *et al.* (1991) to assimilate Geosat data with a variational technique. Kalman filtering is an optimal method which has been recently used by Gaspar and Wunsch (1989) and Fu *et al.*(1991) to assimilate altimetric data in spectral models. They have merely demonstrated the feasibility of the method; their model itself is not realistic enough. In this note, we briefly explore the ability of Kalman filtering in a linear vertical mode model over the entire tropical Atlantic between 10°N and 10°S to describe the variations of sea level. Validation and simulation results are precisely and extensively described in Gourdeau (1991). There we concentrate on the application to actual Geosat data.

The model is described in the next section and the altimetric data processing in the third section, following which we present the assimilation method before finally discussing the results of validation and of assimilation of Geosat data.

THE MODEL AND THE OBSERVATION EQUATION

The model is a simplified version of the linear three-vertical mode model from the Laboratoire d'Océanographie Dynamique et de Climatologie (LODYC) developed for the tropical Atlantic by Arnault (1984) and Levy (1984). As the Kalman filter technique is very cumbersome, if the state vector dimension of the model is too large, we reduce the number of vertical modes from three to one (keeping the second baroclinic vertical mode), and the domain extension to 10°N-10°S (instead of 20°N-20°S). The grid spacing is constant (2° in longitude by 1° in latitude) and pressure and horizontal velocities are computed on an Arakawa type C grid. For such tropical models, no-slip boundary conditions are classically used on coastal and oceanic frontiers. The temporal scheme of the model is a Leapfrog scheme, with a time step of 8 hours. The state vector dimension (n) is about 5 000, corresponding to pressure, zonal and meridional speeds defined twice (due to Leapfrog) at each grid point. The state vector X_k evolves from time step k to k+1 according to the following equation:

$$X_k = AX_k + F_k \qquad (1)$$

where A is the transition matrix representing dynamic laws and F_k is the forcing term. In the present case, the forcing term is represented by wind stress.The model is spun up over four years by the Hellerman and Rosenstein (1983) climatological wind stress, then run with 1985-1988 monthly wind stress derived from ship observations (Servain *et al.*, 1987).

The dynamic height estimate (D) is deduced from the model pressure P through a simple linear relation:

$$D = a + bP \qquad (2)$$

where a and b are constant in time and horizontal space and deduced from the vertical mode (*see* du Penhoat and Treguier, 1985). The dynamic height anomaly (H), our main interest, is computed by substracting from D the annual mean of dynamic height (<D>) issued from the model (H = D - <D>).

The baroclinic character of the tropical ocean permits comparison of dynamic height anomalies (H) with sea level altimetric anomalies (S).

The observation equation relates the variables of the model (X_k) with the observations (Z_k) at instant k.

$$Z_k = H_k X_k \qquad (3)$$

H_k, the observation matrix, has dimensions p*n, n being the state vector dimension and p the observation vector dimension.

There is a bias between the pressure of the model (P) and the altimetric measurement (S). Therefore, data (Z) to be assimilated are along-track values resulting from the addition of the Geosat sea-level anomalies (S) and the local value of the annual mean dynamic height (<D>) of the model minus coefficient a.

$$Z = S + <D> - a \qquad (4)$$

THE ALTIMETRIC DATA

Due to our poor knowledge of the geoid, the reliable satellite altimeter measurements are the sea level anomalies and not the complete signal including the mean sea surface. The Geosat sea-level anomalies have been computed by Arnault *et al.* (1990) for the November 1986-November 1988 period. This data set consists of about 118 repetitive tracks of up to 43 passes each. As noted in the GDR Geosat handbook (Cheney *et al.*, 1987), wet (from FNOC model) and dry tropospheric corrections, ionosphere (GPS model) and tidal signals were removed by Arnault *et al.* (1990). The authors used the colinear profile method (*e. g.*, Menard, 1983) to extract the sea level anomalies that can be decomposed in three steps: 1) The altimetric measurements are resampled along the track at a 60 km spacing; 2) The mean sea level is then calculated and subtracted at each point from each individual profile to produce sea-level anomalies; 3) These anomalies are adjusted with a polynomial least-squares fit to absorb the long wavelength errors. A final smoothing is performed using a median filter over 180 km.

The repetitivity of Geosat is about seventeen days. Two adjacent tracks are separated by 150 km and three days (Fig.1). During the eight-hour time step of the model, no more than four passes can be assimilated. This means that the dimension of the observation vector is never larger than 150.

Figure 1

Representation of the Atlantic basin. The model grid and a three-day sub-cycle Geosat track are shown.

Représentation de la grille du modèle et d'un sous-cycle Geosat sur le bassin atlantique tropical.

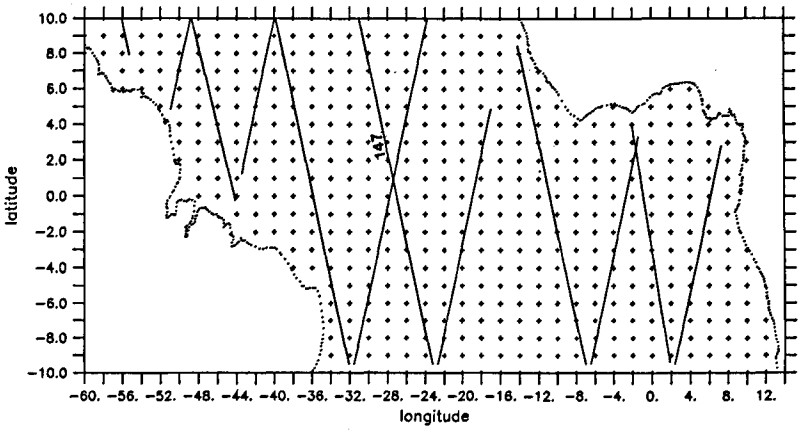

THE KALMAN FILTER

Applied to linear systems, the Kalman filter (Kalman, 1960; Cohn *et al.*, 1981; Miller and Cane, 1989; Gaspar and Wunsch, 1989, Fu *et al.*, 1991) provides the optimal estimation X_k (-,+) of the true state vector X_k, that is a combination of the evolution equation (1) and of all observations up to time k, including (noted +) or excluding (noted -) observations at time k. This estimation is calculated in order to minimize its error variance. A major advantage of this technique is that it provides at every time step the error covariance P_k (-,+) of the estimation. The Kalman filter is a recursive method and results in five equations (Anderson and Moore, 1979). There are two predictive equations which describe the evolution from instant k to instant k +1 of the state vector X and of the associated error covariance P.

$$X_k(-) = A\,X_{k-1}(+) + F_{k-1} \quad (5)$$

$$P_K(-) = AP_{k-1}(+)\,A^T + Q_{k-1} \quad (6)$$

where Q is the error covariance matrix of the model. It represents defects on the physical model (A) and the forcing term (F). It corresponds to errors made during one time-step evolution of the model for prediction of the state vector (X).

A third equation defines the weight matrix K_k, called the "gain matrix", that has to be given to the observations Z_k. The weights defined by the gain matrix depend on the covariance matrices of the model and observation error Q_k and R_k respectively:

$$K_k = P_k\,(-)H_k^T\,(H_kP_k\,(-)\,H_k^T + R_k)^{-1} \quad (7)$$

(where H_k has been defined in equation 4)

The last two equations define the estimate of the state X_k (+) and the associated error covariance P_k (+) after introduction of observation Z_k.

$$X_k(+) = X_k(-) + K_k\,[Z_k - H_kX_k(-)] \quad (8)$$

$$P_k(+) = (I - K_kH_k)\,P_k(-) \quad (9)$$

We assimilate the observations at instant k twice: firstly, on the components of the state X_k (-) from which variables at instant k + 1 are predicted, and secondly on the adjusted estimation of variables at instant k through an Aselin filter (characteristic of a Leapfrog scheme). So, we consider that between two time steps of the model (sixteen hours) observations are not evolving. While doing so, we double the number of observations operating in the estimation of variables at instant k.

ERROR COVARIANCE MATRICES

An important issue to be addressed when using Kalman filters are the various error covariance matrices. They are not easy to estimate, in particular that of the "model". As a first approach, we consider, like Miller and Cane (1989), that the model error is mainly due to errors in the wind forcing. From the tropical wind stress covariance error defined in Miller and Cane (1989), we statistically estimate the effects of random wind stress errors on the state X_k. Variance errors only are computed. They are adjusted according to different tests to form a stationary model error covariance matrix described in Gourdeau (1991).

The errors in the altimetric data are mainly due to error in the satellite orbit computation and uncertainties in the geophysical corrections (troposphere, ionosphere, tides...). An estimation of the observation error covariance due to orbit and wet troposphere along a satellite track has been performed using a new "GEM-T2" satellite orbit (Haines *et al.*, 1990) and a new wet tropospheric correction computed from the SSM/I data (Minster *et al.*, 1992). We first quantified the residual error covariance by comparing the two orbits and the tropospheric corrections [Gourdeau, 1991 (Fig. 2)]. We added to this error covariance estimate an error covariance function and a variance related respectively to the long wavelength tide errors (Benveniste, 1989) and to the instrumental noise (Fig. 2). Finally, the error covariance function of the observations is characterized by a 14 cm2 variance (VO) and a zero crossing around 750 km.

To validate the various error covariance matrices, error variance predicted by Kalman filtering (equations 6, 9) averaged over the basin (VK) are compared with the variance of the difference between Kalman prediction and Geosat observations ($< (H_kX_k\,(-) - Zk)^2 >$) over three days [Geosat sub-cycle (VB), Fig. 3]. VB integrates error variances both of the prediction (VK) and of the observations (VO). A strong value initializes VK, representing the lack of knowledge of the initial state vector (given by the model). VK falls quickly and becomes stationary after forty days with a 10 cm^2 variance. When VO (14 cm^2) is added to VK, a 24 cm^2 variance similar to VB is obtained. This proves the coherence of the error covariance matrices.

The estimated error covariances have been computed by the filter but are not presented here. They oscillate between zero with a seventeen-day period corresponding to the Geosat cycle.

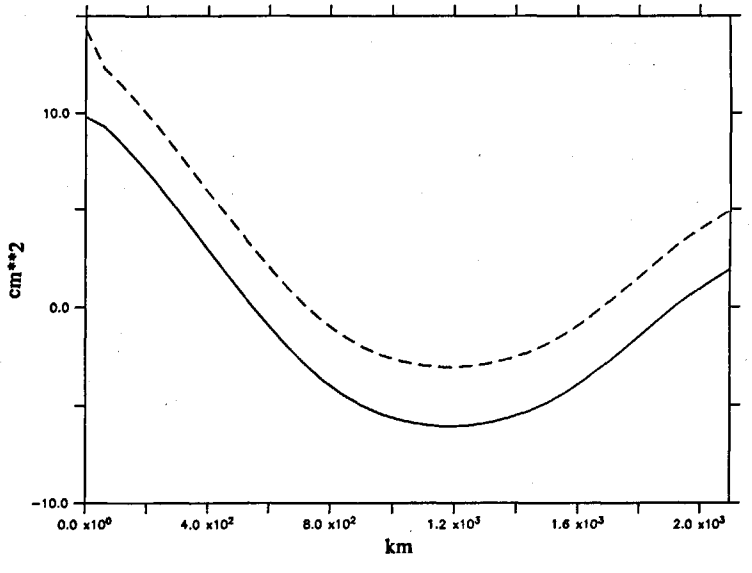

Figure 2

Along-track error covariance function of altimetric data. Only the effects of residual orbit error and wet troposphere error are in solid curve. The complete error covariance corresponding to errors in orbit, wet troposphere, tides and instrumental noise is shown by the dashed curve.

Fonction de covariance d'erreur des données altimétriques le long de la trace. Les contributions de l'erreur d'orbite et de l'erreur de troposphère humide sont en trait continu. Les effets des erreurs de marée et de bruit instrumental ajoutés aux précédentes erreurs définissent la fonction de covariance d'erreur des observations (en trait discontinu).

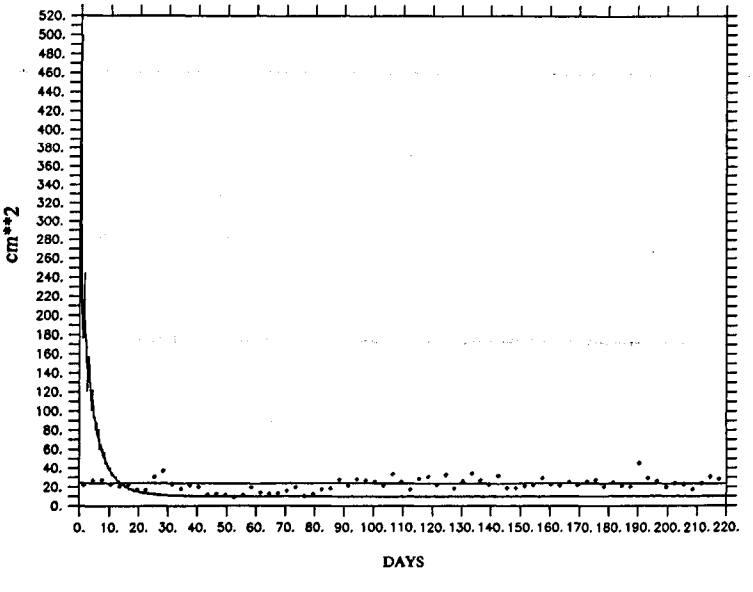

Figure 3

Evolution for the seven-month period of the mean variances from: the errors predicted by the Kalman filter in solid curve (VK); the difference between Geosat data and the state predicted by the Kalman filter in dots (VB). The solid line at 24 cm² corresponds to the estimation of VB, computed by addition of VK and the error variance of the observations (VO).

Évolution pour les sept mois d'assimilation de la variance moyenne calculée pour : a) l'erreur prédite par le filtre de Kalman [VK (en trait continu)] ; b) la différence entre les données Geosat et l'état prédit par le filtre de Kalman [VB (points noirs)]. Le trait continu à 24 cm² correspond à l'estimation de VB calculée en ajoutant à VK la variance d'erreur des observations (VO).

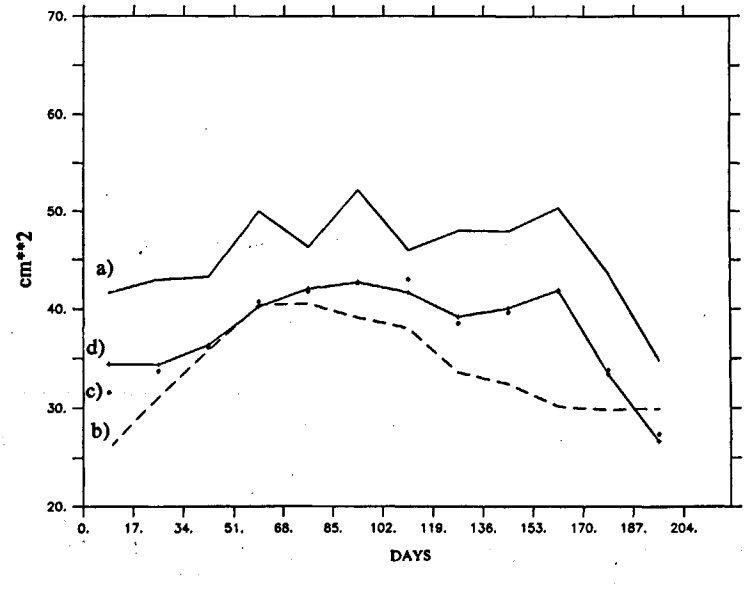

Figure 4

Evolution for the seven-month period of assimilation of variances averaged every seventeen days along every satellite track computed from: a): Geosat observations; b): model; c): predicted state X (-); d): analysed state X (+)

Évolution pour les sept mois d'assimilation des variances : a) des observations Geosat ; b) de l'état du modèle sans assimilation ; c) de l'état prédit par le filtre X (-) ; d) de l'état analysé par le filtre X (+). Les variances sont moyennées tous les 17 jours le long des traces satellites.

RESULTS AND DISCUSSION

As far as computer developments are concerned, the programme is implemented on a CRAY2 computer and a one-month assimilation requires seven hours of computing time.

Experiments of sensitivity and behaviour of the filter have been performed with simulated data (Gourdeau, 1991).

They are not presented here. The most significant of these was the assimilation of simulated data obtained by sampling an OGCM along the Geosat tracks (Morlière *et al.*, 1989) with a realistic altimetric noise added. Results were convincing enough to start assimilation of real Geosat data (Gourdeau, 1991). These data were assimilated over a seven-month period, from January to July 1987.

A perfect model would explain all of the observed variance not due to noise. The maximum possible extent to which the model can describe the observation level is the question to be answered. The total variance of the Geosat observations is estimated to 44.8 cm^2, of which 14 cm^2 is due to observation errors, leaving 30.8 cm^2 for the signal variance. The Kalman prediction, which uses only the "prior observations", is characterized by a total variance of 37.1 cm^2, 10 cm^2 of which represent the estimated error variance (VK). So, the filter recovers a signal variance of 27.1 cm^2, corresponding to 87 % of the observed signal variance. Therefore, from a statistical point of view, our linear model seems particularly appropriate to assimilate Geosat observations of the tropical Atlantic Ocean. Note that Fu *et al.* (1991), through their Kalman filtering experiences in the tropical Pacific, only explain 23 % of the signal variance.

The evolution of the predicted field variance averaged for every 17-day-period is coherent with the Geosat "observation" (Fig. 4). The maximum of signal is in March 1987 when the wind speed in the northern hemisphere is strong. The variance of the model is not so far from the others but decreases in April 1987 against June 1987 for Geosat observations and the solution predicted by the Kalman filter.

The validation of the Kalman filter requires the comparison of solutions obtained by the filter with independent observations. For this, we compare the predicted state $X_k(-)$ with the Geosat observations along track 147 at every 17-day period (Fig. 5 *a*). We see that both predicted and Geosat signals seem rela-

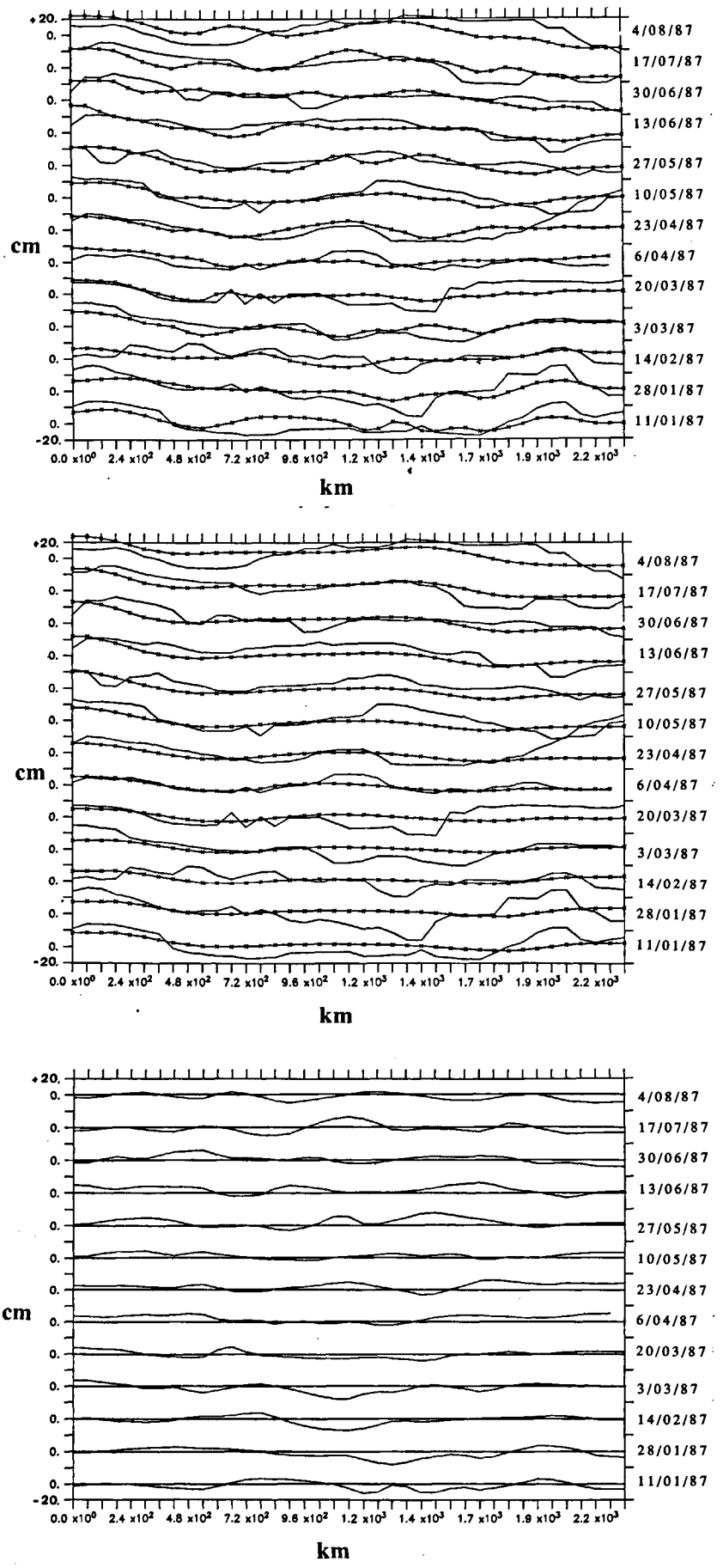

Figure 5

Evolution along track 147 (shown in Fig. 1) of the prediction and Geosat observations (5 a*); benchmark and Geosat observations (5* b*), and of the difference between prediction and benchmark (5* c*). Geosat observations are in solid line, prediction and bechmark are in solid line with cross.*

Évolution temporelle le long de la trace 147 (localisée sur la fig. 1) des observations Geosat et de l'état prédit par le filtre (5 *a*) ; des observations Geosat et de l'état du modèle sans assimilation (5 *b*) ; et de la différence entre l'état prédit par le filtre et l'état du modèle sans assimilation (5 *c*). Les observations Geosat sont en trait continu. L'état prédit par le filtre et l'état du modèle sans assimilation sont en trait continu avec les croix.

Figure 6

a: Climatological dynamic topography anomalies for March (DH); b: dynamic topography anomalies (in centimetres) for March 1987 estimated by objective analysis of altimetry (AL); c: three vertical mode model results (3M); d: three-dimensional model results (3D); e: simplified one-mode model as benchmark (BM); f: assimilation results (AS). Positive values are in solid lines (panels e and f) or light grey color (panels a-d), negative values are in dashed lines (panels e and f) or heavy grey color (panels a-d). Figures a *to* d *are from Arnault* et al. *(1991).*

Cartes mensuelles d'anomalies de topographie dynamique pour le mois de mars 1987 issues : a) de la climatologie (DH) ; b) de l'analyse objective des données altimétriques (AL) ; c) du modèle linéaire à trois modes verticaux (3 M) ; d) du modèle tridimensionnel (3 D) ; e) du modèle linéaire à un mode servant à l'assimilation (BM) ; f) de l'assimilation par le filtre de Kalman (AS). Les unités sont en centimètres. Les figures *a, b, c, d* proviennent de Arnault *et al.* (1991).

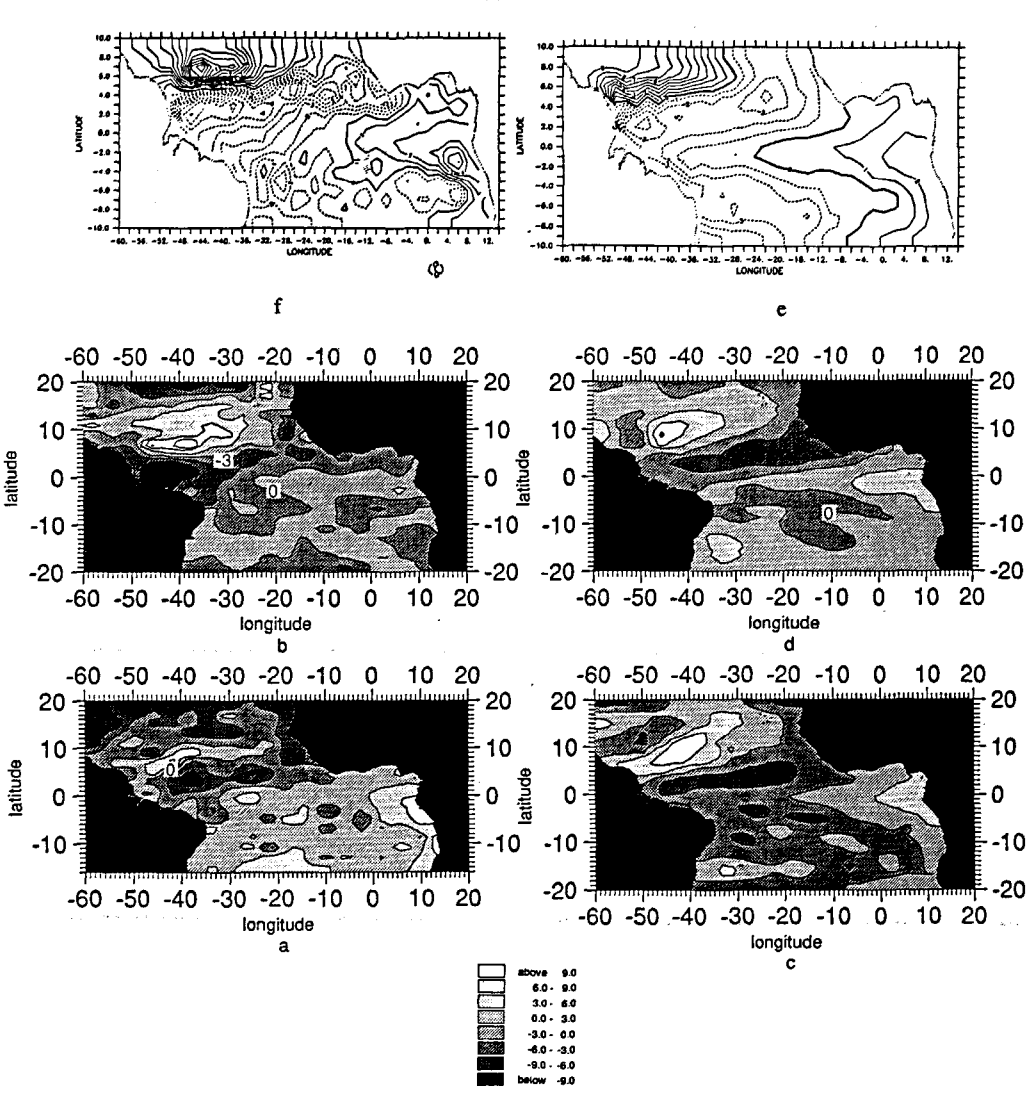

tively similar if we consider that Geosat obervations are noisy. We also see a good agreement between the benchmark and Geosat observations (Fig. 5 *b*), but the benchmark presents a very smooth signal. The difference between the predicted state and the benchmark (Fig. 5 *c*) represents the part of the signal in the observations that is assimilated in the model and not present in the benchmark. We observe variations with an amplitude of the order of 5 centimetres.

We compare the results of the assimilation (AS hereafter) with five other products. This was done for two months: March 1987 and June 1987 - which are characteristic of the seasonal cycle in the tropical Atlantic (Merle and Arnault, 1985). The first comparison, of course, is the benchmark (BM), *i. e.* the model run without assimilation. The second consists in the results of the three-vertical mode model, as run by Arnault *et al.* [1990 (3M hereafter)]. The other modelled product is from the 3D model (3D), forced with monthly 1987-1988 wind stresses (Morlière *et al.*, 1989). Altimetric sea surface topography anomalies mapped with an objective analysis by Arnault *et al.* [1991 (AL hereafter)], and climatological dynamic height (DH; Merle and Arnault, 1985) are the other sets in this model results/data comparison. The objective analysis algorithm (De Mey and Robinson, 1987) was derived from an analytical correlation function described by:

$$f = [1 + R\,(1 + R/3)] * \exp(-R) * \exp(-t^2/rct^2) \qquad (10)$$

with R = cste * r/rcx (cste = 2.1), where r is the distance and t is the time separating the interpolated point and any point in the influence radii areas. Values of 500 km and 140 days were chosen for space and time decorrelation scales (rcx and rct). The influence radii that fix the space-time size of the interpolation domain are 300 km and thirty days. The associated error variances correspond to 30 % of the observation variances and the background field for the optimal analysis is zero (Arnault *et al.*, 1990).

The dynamic topography anomalies in the tropical Atlantic present series of mostly zonal patches of alternatively positive or negative sign.

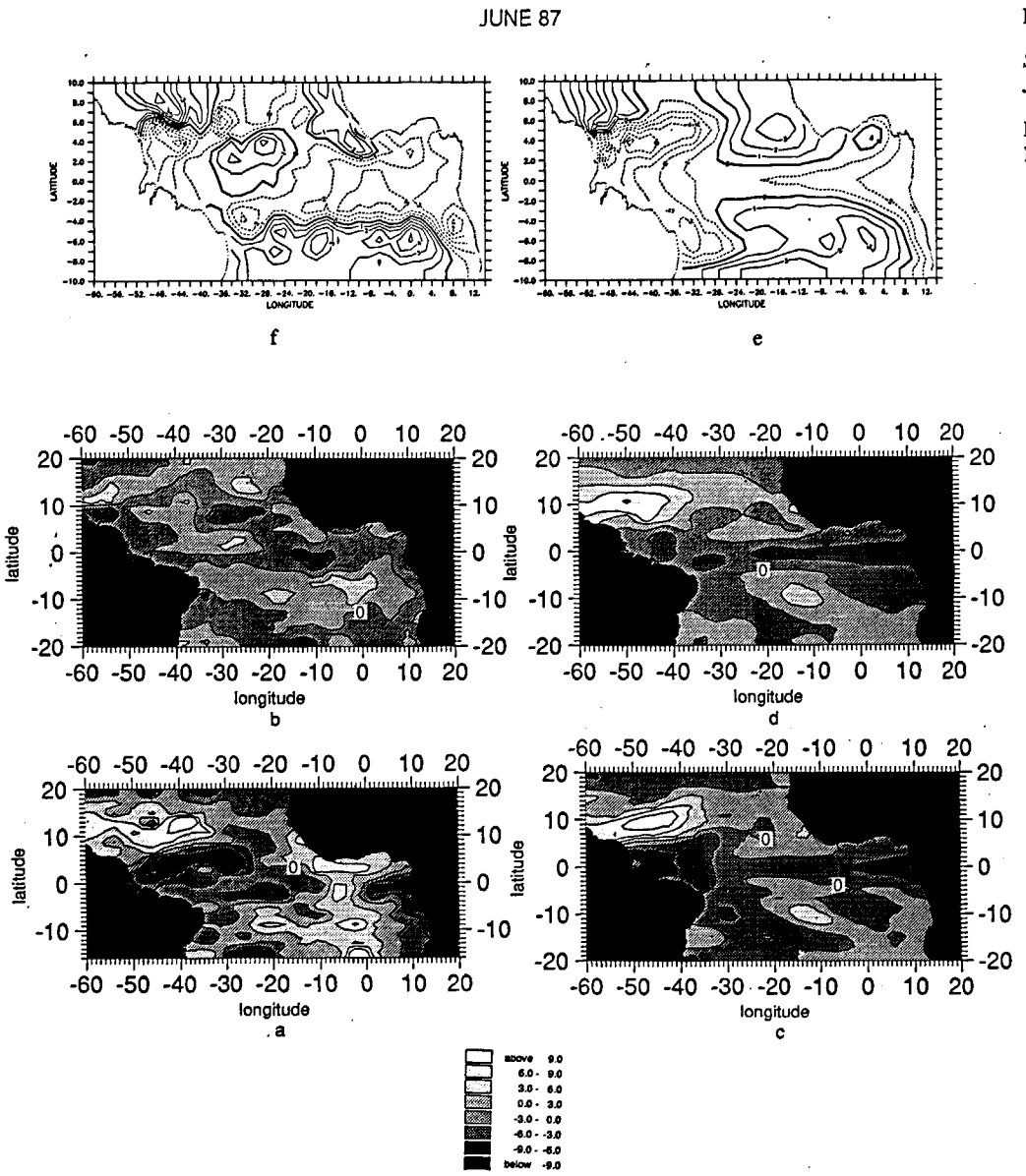

Figure 7

Same as in Figure 6 except for June 1987.

Identique à la figure 6, sauf pour le mois de juin 1987.

First, if one looks merely at the models without assimilation and objective analysis of the data in March 1987 (Fig. 6), it may be seen that the North Equatorial Counter Current (NECC) region is characterized by negative values around 6 cm in the 3D, 3M, DH and AL maps. Due to its simplified version, reduced to one mode, the BM signal only reaches 3 cm. Further north, the signal is positive (around 8 cm) for all fields. In the Gulf of Guinea, the main disagreement occurs between AL and the other results: latter show positive values of about 3 cm while AL does not present any significant signal. Tai (1991) has studied the effect of track length for the polynomial orbit error correction, according to the along-track signal wavelength. For short wavelength signal, he shows that an important fraction is filtered for short track length. This situation is applicable in the Gulf of Guinea where, due to the continental coastline, tracks are short and where at the equator, meridional signal structures also are short. Looking at the AS results now, one can see that in the NECC region, the Geosat observations greatly improve the computation. Stronger signal is now restored, in good agreement with AL, 3D, 3M and DH. On the other hand, in the Gulf of Guinea, where the Geosat data are suspect, the dynamic of the model seems decisive in order to restore the signal. In that case, the advantage of the model as a data interpolator (or propagator) is clear.

In June 1987 (Fig. 7), things are similar except that, due to upwelling in the Gulf of Guinea, the signal changes sign and is negative, about - 5 cm for 3D, 3M and DH. Due to the data filtering problems as mentioned above and to the simplified model, AL and BM only reach - 2 cm. The NECC starts to increase so that the negative anomaly in that region also weakens. In addition AL presents a shift of about one month compared to 3D, 3M, BM or DH. AS improvements here are again significant: First, the observations restore the early NECC increase. Second, the equatorial upwelling signal is more significant, although an amplitude difference always exists. In order to solve the poor energetic signal of data in the Gulf of Guinea, new treatments are being applied on Geosat altimetric measurements at the GRGS group in Toulouse.

CONCLUSION

It may be concluded that assimilation techniques, such as the Kalman filter, allows a simple model to fit Geosat altimetric data. We restore 87 % of the signal observation variance that confirms the choice of a simple linear model. The good efficiency of Geosat observations as a constraint of the model is clearly shown in the western part of the basin whereas in the gulf of Guinea, where altimetric data are doubtful, the dynamic of the model is able to reproduce a more realistic signal.

This work will serve as a basis for evaluating the performance of degraded Kalman filters.

Improvements have still to be made in the manner of implementation of oceanic data assimilation, but preliminary works such as that presented here underline the great potential apparently offered to oceanographers by merging satellite data and models.

Acknowledgements

This research has been funded by the French Programme National de Télédetection Spatiale (PNTS). Special thanks to J.-F. Minster and the GRGS group for welcoming L. Gourdeau to their laboratory. L. Gourdeau, S. Arnault and J. Merle were supported by ORSTOM (Institut Français de Recherches Scientifiques pour le Développement en Coopération) and Y. Ménard by the Centre National d' Études Spatiales.

REFERENCES

Anderson B.D.O. and J.B. Moore (1979). *Optimal filtering*, Prentice-Hall, Englewood Cliffs, 357 pp.

Arnault S. (1984). Variation de la topographie dynamique et de la circulation superficielle de l'Océan Atlantique tropical. *Thèse de Doctorat 3ème cycle; Université Pierre et Marie Curie, Paris, France.*

Arnault S. and C. Périgaud (1992). Altimetry and models in the tropical ocean: a review. *Oceanologica Acta*, **15**, 5, 411-430 (this issue).

Arnault S., Y. Ménard and J. Merle (1990). Observing the tropical Atlantic Ocean in 86-87 from altimetry. *J. geophys. Res.*, **95**, C10, 17921-17945.

Arnault S., A. Morlière, Y. Ménard and J. Merle (1991). Low frequency variability of the tropical Atlantic surface topography: altimetry and models comparison. *J. geophys. Res.* (in press).

Benveniste J, (1989). Observer la circulation des océans à grande échelle par altimétrie satellitaire, *Thèse, Université P. Sabatier, Toulouse, France*, 198 pp.

Bourles B., S. Arnault and C. Provost (1991). Toward altimetric data assimilation in a tropical Atlantic model. *J. geophys. Res.* (in press).

Carton J.A and E.C. Hackert (1990). Data assimilation applied to the temperature and circulation in the tropical Atlantic, 1983-1984. *J. phys. Oceanogr.*, **20**, 1150-1165.

Cheney R.E., B.C. Douglas, R.W. Agreen, L.L. Miller and D.L. Porter (1987). Geosat Altimeter Geophysical Data Record (GDR) user handbook, National Ocean Survey/NOAA, 23 pp.

Cohn S., M. Ghil and E. Isaacson (1981). Optimal interpolation and the Kalman filter. *Fifth Conference on Numerical Weather Prediction, American Meteorological Society, Boston, MA 02108, USA*, 36-42.

De Mey P. and, A.R. Robinson (1987). Simulation and assimilation of satellite altimeter data at the oceanic mesoscale. *J. phys. Oceanogr.*, **17**, 2280-2293.

Derber J. and A. Rosati (1989). A global oceanic data assimilation system. *J. phys. Oceanogr.*, **19**, 1333-1347.

du Penhoat Y. and A.-M. Treguier (1985). The seasonal linear response of the tropical Atlantic Ocean. *J. phys. Oceanogr.*, **15**, 316-329.

Fu L.L., J. Vazquez and C. Périgaud (1991). Fitting dynamic models to the Geosat sea-level observations in the tropical Pacific Ocean. Part 1: A free wave model. *J. phys. Oceanogr.*, **21**, 798-808.

Gaspar P. and C. Wunsch (1989). Estimates from altimeter data of barotropic Rossby waves in the northwestern Atlantic Ocean. *J. phys. Oceanogr.*, **19**, 1821-1844.

Gourdeau L. (1991). Application du filtrage de Kalman à l'assimilation de données altimétriques dans un modèle linéaire de l'océan Atlantique tropical. *Thèse, Université Pierre.et Marie Curie, Paris, France*, 270 pp.

Haines B.J, G.H. Born, G.W. Rosborough, J.G. Marsh, R.G. Williamson (1990). Precise orbite computation for the Geosat exact repeat mission. *J. geophys. Res.*, **95**, 2871-2886.

Hellerman S. and M. Rosenstein (1983). Normal monthly wind stress over the world ocean with error estimates. *J. phys. Oceanogr.*, **13**, 1093-1104.

Kalman R.E. (1960). A new approach to linear filtering and prediction problems. *J. basic Eng., Trans. ASME, Ser. D.*, **82**, 35-45.

Leetma A. and M. Ji (1989). Operational hindcasting of the tropical Pacific. *Dynam. Atmos. Oceans*, **13**, 465-490.

Lévy C. (1984). Modélisation numérique du cycle saisonnier de l'Océan Atlantique tropical: rôle des fronts de vent. *Thèse, Université Paris VI, France.*

Ménard Y. (1983). Observation of eddy fields in the northwest Pacific by Seasat altimeter data. *J. geophys. Res.*, **88**, 1853-1866.

Merle J. and S. Arnault (1985). Seasonal variability of the surface dynamic topography in the tropical Atlantic Ocean. *J. mar. Res.*, **43**, 267-288.

Miller R.N.and M.A. Cane (1989). A Kalman filter analysis of sea-level height in the tropical Pacific. *J. phys. Oceanogr.*, **19**, 773-790.

Minster J.-F., D. Jourdan, E. Normant, C. Brossier and M.C. Genero (1992). An improved SSM/I water vapor correction for Geosat altimeter data. *J. geophys. Res.* (in press).

Moore A.M, N.S. Cooper and D.L.T. Anderson (1987). Initialisation and data assimilation in models of the Indian Ocean. *J. phys. Oceanogr.*, **17**, 1965-1977.

Morlière A., G. Reverdin and J. Merle (1989). Assimilation of temperature profiles in a general circulation model of the tropical Atlantic. *J. phys. Oceanogr.*, **19**, 1892-1899.

Philander G.S.H. and R.C. Pacanowski (1986). A model of the seasonal cycle in the tropical Atlantic Ocean. *J. geophys. Res.*, **91**, 14192-14206.

Scheinboum J. and D.L.T. Anderson (1990). Variational assimilation of XBT data. Part 1. *J. phys. Oceanogr.*, **20**, 672-688.

Schott F.A. and C.W. Boning (1991). The WOCE model in the western equatorial Atlantic: upper layer circulation. *J. geophys. Res.*, **96**, 6993-7004.

Servain J., M. Serva, S. Lukas and G. Rougier (1987). Climatic atlas of the tropical Atlantic wind stress ans sea surface temperature 1980-1984. *Ocean-air Interactions*, **1**, 109-182.

Tai C.-K. (1991). How to observe the gyre to global-scale variability in satellite altimetry. *J. atmos. ocean Technol.*, **8**, 272-288.